Observation of persistent -helical content and discrete types of backbone disorder during a molten globule to ordered peptide transition via deep-UV resonance Raman spectroscopy

ARTICLE *in* JOURNAL OF RAMAN SPECTROSCOPY · JULY 2013

Impact Factor: 2.67 · DOI: 10.1002/jrs.4316

5 AUTHORS, INCLUDING:

Jason W Cooley
University of Missouri
36 PUBLICATIONS **506** CITATIONS
SEE PROFILE

Andrew Mutter
Harvard University
11 PUBLICATIONS **37** CITATIONS
SEE PROFILE

Renee D. Jiji
University of Missouri
38 PUBLICATIONS **388** CITATIONS
SEE PROFILE

Ronald Koder
City College of New York
46 PUBLICATIONS **795** CITATIONS
SEE PROFILE

Research article

Journal of RAMAN SPECTROSCOPY

Received: 10 January 2013 Revised: 3 April 2013 Accepted: 8 April 2013 Published online in Wiley Online Library

(wileyonlinelibrary.com) DOI 10.1002/jrs.4316

Observation of persistent α-helical content and discrete types of backbone disorder during a molten globule to ordered peptide transition via deep-UV resonance Raman spectroscopy

Mia C. Brown,[a] Andrew C. Mutter,[b†] Ronald L. Koder,[b†] Renee D. JiJi[a] and Jason W. Cooley[a]*

The molten globule (MG) state can aid in the folding of a protein to a functional structure and is loosely defined as an increase in structural disorder with conservation of the ensemble secondary structure content. Simultaneous observation of persistent secondary structure content with increased disorder has remained experimentally problematic. As a consequence, modeling how the MG state remains stable and how it facilitates proper folding remains difficult due to a lack of amenable spectroscopic techniques to characterize this class of partially unfolded proteins. Previously, deep-UV resonance Raman (dUVRR) spectroscopy has proven useful in the resolution of global and local structural fluctuations in the secondary structure of proteins. In this work, dUVRR was employed to study the MG to ordered transition of a model four-helix bundle protein, HP7. Both the average ensemble secondary structure and types of local disorder were monitored, without perturbation of the solvent, pH, or temperature. The MG to ordered transition is induced by stepwise coordination of two heme molecules. Persistent dUVRR spectral features in the amide III region at 1295–1301 and 1335–1338 cm^{-1} confirm previous observations that HP7 remains predominantly helical in the MG *versus* the fully ordered state. Additionally, these spectra represent the first demonstration of conserved helical content in a MG protein. With successive heme binding, significant losses are observed in the spectral intensity of the amide III_3 and S regions (1230–1260 and 1390 cm^{-1}, respectively), which are known to be sensitive to local disorder. These observations indicate that there is a decrease in the structural populations able to explore various extended conformations with successive heme binding events. DUVRR spectra indicate that the first heme coordination between two helical segments diminishes exploration of more elongated backbone structural conformations in the inter-helical regions. A second heme coordination by the remaining two helices further restricts protein motion.

Keywords: dUVRR, deep-UV resonance Raman spectroscopy; tertiary structure; secondary structure; structural disorder; molten globule

Introduction

Protein stability at the level of tertiary structure can play a significant role in the equilibrium between a fully functional protein and various denatured or unfolded states. The molten globule (MG) state is a metastable structure first put forth in 1981 as a model to explain rapid refolding of α-lactalbumin to the native globular state.[1] The formal characteristics of an MG state include conservation of native secondary structure and loss of tertiary structural interactions, such as close packing of side chains and disulfide linkages. There is a high degree of cooperativity in the unfolding process from the MG to completely unfolded state, allowing for many smaller structural fluctuations, but keeping the protein in a native-like state.[2,3] These small structural fluctuations are thought to stabilize MG proteins in varying local environments.[4] The existence of the MG state has since been conclusively confirmed by various means[5,6] and shown to play an important role in biological functions,[4] including protein–membrane and protein–ligand interactions, cell transport, and folding–unfolding pathways.[7–12]

The MG's inherent flexibility makes structural analysis by X-ray crystallography impossible. Nuclear magnetic resonance (NMR) spectroscopy offers the most detailed structural information on globular proteins,[13–21] but interpretation is complicated by broad resonances and small dispersions in MG protein spectra.[3] Lower resolution methods such as circular dichroism (CD) and infrared spectroscopy are thus the predominant tools for the study of MG proteins because they offer snapshots of structural changes.[22–32] However, these techniques generally yield information on either secondary or tertiary structural interactions, but not both simultaneously. Additionally, when using these spectroscopic techniques, persistent secondary structure in the MG state is inferred from the deconvolution of broad, featureless spectral signals, making direct assessment of structural content tenuous.

* *Correspondence to: Jason W. Cooley, Department of Chemistry, University of Missouri, Columbia, MO 65211, USA.E-mail: cooleyjw@missouri.edu*

† *These authors contributed equally*

a *Department of Chemistry, University of Missouri, Columbia, MO 65211, USA*

b *Department of Physics, The City College of New York, New York, NY 10031, USA*

Deep-UV resonance Raman (dUVRR) spectroscopy is a method wherein the vibrational modes of the peptide backbone and aromatic residues are probed in order to elucidate structural characteristics of a protein. Owing to the increased number of well-resolved peptide backbone vibrational modes visible by dUVRR spectroscopy, a broad array of studies pertaining to secondary structure content and changes using resonance Raman spectroscopy have been published previously.[33–37] Previous resonance Raman studies on changes in tertiary structure have been limited to far-UV and visible excitation.[25,38–41] One example is Hildebrandt *et al*., where Soret band excitation of the heme cofactor was used to examine the integrity of the heme binding crevice of cytochrome *c* upon binding to cytochrome oxidase.[25] While this study established that resonance Raman spectroscopy can be used to probe changes in tertiary structure, the use of a cofactor and its region of excitation severely limit the information that can be obtained for other proteins. Currently, it remains unclear to what extent dUVRR spectroscopy is useful for studying changes in the tertiary structure of native proteins.

The dUVRR spectra of proteins are correlated with the global secondary structure content of proteins. In addition, the position of the amide III mode has been shown to be dependent on the ψ dihedral angles of the peptide backbone.[42–44] Thus, there is a strong likelihood that dUVRR spectra will report on changes in tertiary structure as well. There are manifold advantages to using Raman spectroscopy, not least of which is the ability to use water as a solvent, as it is a weak Raman scatterer. The ability to analyze molecularly complex protein samples, such as those associated with membrane bilayers, is an additional advantage.[45] To test the amenability of dUVRR spectroscopy to monitor tertiary structure fluctuations and their consequences on local secondary structure, we have chosen to study the de novo synthesized peptide, HP7, an ideal candidate for studies in this area. The four-helical bundle peptide maintains its α-helical secondary structure while its tertiary structure depends upon the stoichiometric binding of heme molecules. In the absence of heme prosthetic groups, HP7 resides in an MG state. Upon stoichiometric heme addition and binding between each pair of helices, the protein adopts a more rigid, more ordered conformation, as judged by NMR.[46] Thus, we can observe the transition from an ordered tertiary state to an MG in a controlled manner. Here, we describe the first use of dUVRR spectroscopy as the analytical method for measuring tertiary disorder of a protein, documenting for the first time unambiguous persistence of the global secondary structure content in an MG state.

Materials and methods

Sample preparation

^{15}N labeled HP7 was generated as a recombinant protein and purified by centrifugation from lysate of *E. coli* cells grown in ^{15}N rich media. ^{15}N labeling was originally carried out to facilitate NMR analysis. Analytical ^{18}C high-performance liquid chromatography was used to confirm the purity of the protein. The apo-HP7 (AHP7) protein sample (43.55 μM) was prepared in 25 mM borate buffer (pH 9.5). UV–Vis spectral intensity at 280 nm was used to determine protein concentration. Aliquots of the AHP7 were set aside and heme from a 2.1 mM stock solution in dimethyl sulfoxide (DMSO) were added step-wise in one-fifth equivalents (8.71 μM) to obtain the half-heme (HHP7) and fully bound heme (FHP7) samples. The DMSO was removed by dialysis against a 25 mM borate buffer at pH 9.5. $NaClO_4$ was added to each sample as an internal intensity standard from a stock solution to a final concentration of 50 mM.

N-methylacetamide (NMA) was obtained from Sigma (St. Louis, MO), and ^{15}N labeled NMA was obtained Cambridge Isotopes (Andover, MA). NMA samples (5 mg ml^{-1}) were prepared in 20 mM phosphate buffer (pH 7). $NaClO_4$ was added to the NMA sample as an internal intensity standard from a stock solution to a final concentration of 50 mM.

CD

CD spectra were collected on a Jasco J-815 CD spectropolarimeter (Easton, MD) using a Hellma cuvette with a pathlength of 1 mm. The protein concentrations were 43.55 μM in a buffer of 25 mM borate and 50 mM $NaClO_4$ (pH 9.5).

dUVRR

The dUVRR instrument was set up as described previously.[47] Briefly, the fourth harmonic of a titanium-sapphire laser at an excitation wavelength of 197 nm was directed onto a thin film of sample flowing between two nitinol wires spaced approximately 1 mm apart under N_2 gas. The incident laser power at the sample was attenuated to 500 μW to avoid protein degradation, and spectra were monitored for degradation over time using the aromatic ring modes. Spectra were collected over 4 h. Spectral calibration was carried out using a standard cyclohexane spectrum.[48] All dUVRR spectral preprocessing was carried out in MATLAB (7.1, MathWorks, Natick, MA) using cosmic ray and water band removal methods described previously.[49] A nonlinear least-squares algorithm was used to fit the amide and aromatic bands to mixed Gaussian/Lorentzian peaks, which approximate the Voigt line shape as described previously.[50]

Results

Changes in the CD spectra of HP7 with heme content

The CD spectrum of the AHP7 protein exhibits two minima at 205 and 222 nm, consistent with the interpretation that the MG form of the peptide retains significant helical character despite lack of heme coordination (Fig. 1). The intermediate HHP7 protein displayed a somewhat less intense minimum at 207 nm and a slightly more intense minimum at 222 nm, consistent with the loss of some of the disordered structure (Fig. 1).[22,28,29,51–53] The CD

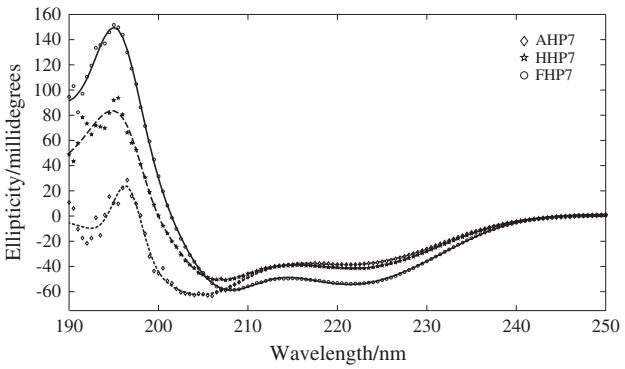

Figure 1. Far UV circular dischroism spectra of HP7 with various heme stoichiometries. Representative CD spectra of AHP7, HHP7, and FHP7 reveal a distinct change.

Journal of RAMAN SPECTROSCOPY

spectrum of the FHP7 sample exhibits a classically α-helical shape, with two minima at 209 and 222 nm and a maximum at 199 nm (Fig. 1).

Influence of ^{15}N labeling on backbone amide vibrational modes

In order to assign the amide mode changes associated with the MG to ordered transition of the ^{15}N labeled HP7 protein, we first characterized the influence of ^{15}N labeling on NMA, a simple model for a peptide backbone. Upon ^{15}N labeling of the NMA molecule, the amide I (predominantly C=O stretching)[33,54] and amide S (in-plane N–H/C–H coupled bending)[55] associated Raman shift positions are unchanged (Fig. 2). The amide I position (1651 cm^{-1}) was determined using a fit of the amide I region and is slightly higher than that previously reported by Chen *et al*.[56] with 244 nm excitation. This difference is likely not significant due to the low intensity of the amide I band of NMA with deep-UV excitation.[54] Conversely, the amide II band (predominantly N–H bending)[57] is red-shifted by as much as 17 cm^{-1}, and the amide III band (C–N stretching/N–H bending and stretching) also undergoes a small redshift (3 cm^{-1})[55] in the dUVRR spectrum upon isotopic labeling (Fig. 2). Therefore, one would expect subtle differences in the amide II and III bands from those of an unlabeled protein dUVRR spectrum upon incorporation of ^{15}N in the peptide backbone.

Based upon the shifts in the assignment of the ^{15}N labeled NMA, the ^{15}N labeled HP7 amide backbone spectral contributions are straightforward to assign. DUVRR spectra were collected for the three forms of HP7, and then the line shape was fit using a nonlinear least squares algorithm as described previously[58] to understand the contributing vibrational modes (Fig. 3). The amide I band can be adequately modeled in each case with a single component with a maximum at 1668 cm^{-1}. Two features are

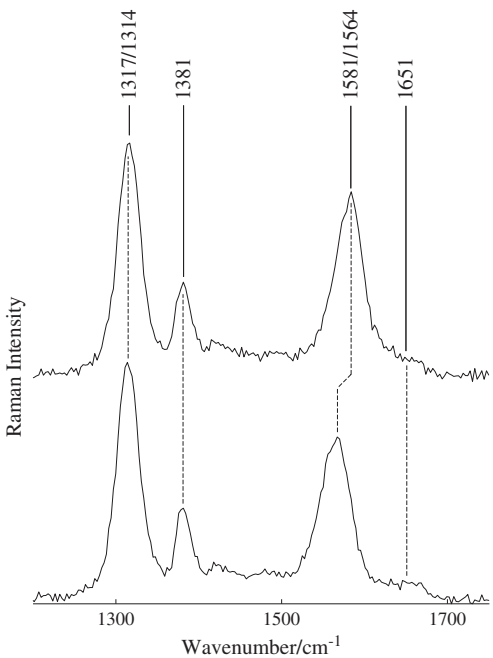

Figure 2. Assignment of vibrational modes upon ^{15}N labeling of *N*-methylacetamide (NMA). Representative dUVRR of NMA (upper trace) and 15NMA (lower trace) amide modes with corresponding Raman shift assignments (dashed vertical lines).

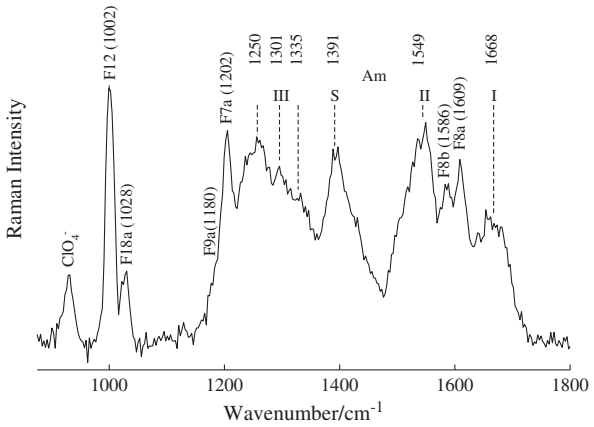

Figure 3. DUVRR spectrum and mode assignmnets for HP7 without added heme. Backbone amide mode assignments are indicated with the standard numerals I, II, III, and S. Features consistent with contributions from the aromatic vibrations of phenylalanine are indicated with its single letter notation (F) and a numeral corresponding to the accepted nomenclature for the wavenumbers' origin.

required to model the amide II band: 1513/1504/1501 and 1549/1544/1538 cm^{-1} for the AHP7, HHP7, and FHP7 samples, respectively. This is phenomenologically similar to previous studies of predominantly helical proteins, but with slightly red-shifted wavenumbers. The amide S was modeled with peaks at 1391/1391/1394, again for AHP7, HHP7, and FHP7, respectively. Three contributions for AHP7, HHP7, and FHP7 at 1250/1245/1250, 1301/1293/1295, and 1335/1338/1338 cm^{-1} are required to fit the amide III region, which is also consistent with Raman shifts described previously for the amide III region.[59] While there are subtle differences in the shift of the maxima of the fitted bands from one structural form to the next, the primary differences in the spectra lie in the intensity of the individual spectral features.

DUVRR spectra of HP7 as a function of heme content

Unlike the broad and featureless spectral changes associated with heme binding in the HP7 CD spectra, the dUVRR spectra have reasonably well-resolved spectral features that report independently on changes in the local protein structure and the local environment of the backbone. There is no contribution from protoporphyrin-related modes in UVRR spectra.[38–40] Despite the similar Raman shift positions for all of the dUVRR spectral features in the three forms of HP7, the intensities of the modes changed significantly with heme binding. Specifically, the amide II (1545 cm^{-1}), III (1250 cm^{-1}), and S (1390/1450 cm^{-1}) bands all decreased in intensity with heme binding (Fig. 4). Conversely, the intensity of the amide III bands at 1301 and 1335 cm^{-1}, which are conserved in dUVRR spectra of helical proteins,[50,55,58] is unchanged in all the three states (Fig. 4).

Studies by Asher and coworkers[44,60,61] have shown that the lowest wavenumber amide III mode is dependent on the ψ dihedral angle. This mode is commonly referred to as the amide III_3 mode. Difference spectra of the amide III_3 region consecutively showed two distinct changes with each heme binding (Fig. 5). The amide III_3 shift can be used to predict the ψ angle to within ±8° using Eqn (1)[44]:

$$\vartheta_{III3}^{EXT} = \left[1256\ cm^{-1} - 54\ cm^{-1} sin(\psi + 26^{\circ})\right] - 0.11\frac{cm^{-1}}{^{\circ}C}(T - T_0) \quad (1)$$

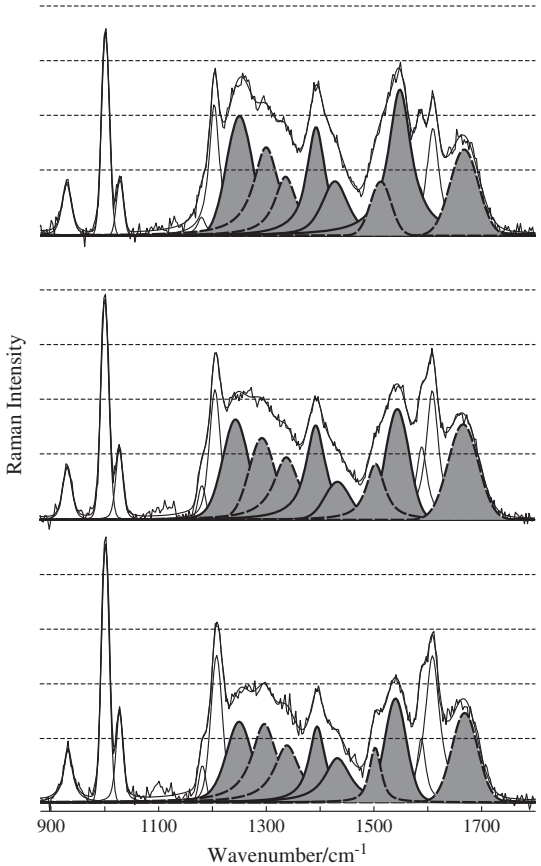

Figure 4. DUVRR analysis of structural changes upon successive heme addition. DUVRR spectra of AHP7 (upper), HHP7 (middle), and FHP7 (lower) are presented, as well as non-linear least squares spectral fitting results for each. Contributions arising from peptide backbone amide modes are indicated with filled curves, while those also corresponding α-helix associated wavenumbers are further delineated with dashed lines.

As there is only a 3 cm^{-1} shift in the $AmIII_3$ due to isotopic labeling, all ψ dihedral angle values from Eqn (1) will fall within error of values obtained without isotopic labeling. From these calculations, it is apparent that each heme binding event results in a structural transition. When the HHP7 spectrum is subtracted from that of the AHP7, the resulting feature in the difference spectrum occurs at approximately 1265 cm^{-1}, which corresponds to a ψ angle of 166°, consistent with extended-strand like structure.[61] When the FHP7 spectrum is subtracted from the HHP7 spectrum, the remaining feature occurs at approximately 1233 cm^{-1}, corresponding to a ψ angle of 132°, more consistent with extended helical or polyproline II type structure.[44]

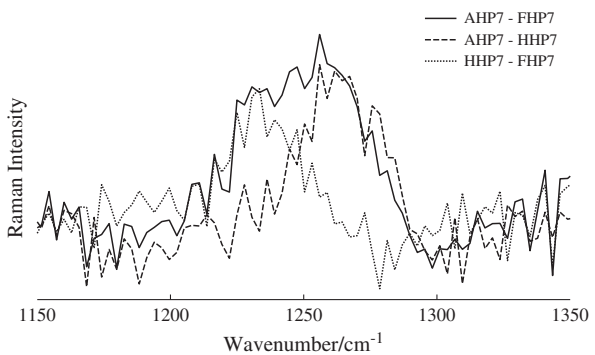

Figure 5. Changes in the amide III_3 region of HP7 upon heme addition. The AHP7 minus, FHP7, AHP7 minus HHP7, and HHP7 minus FHP7 difference spectra of the amide III[3] region.

Discussion

Persistent helical content from ordered to MG states

CD spectra of both forms of HP7 display the same local minimum at 222 nm, indicating that they contain approximately the same amount of α-helical secondary structure. This interpretation is supported by the dUVRR spectra of AHP7, HHP7, and FHP7. Specifically, the amide III bands at 1301 cm^{-1} and 1335 cm^{-1} are consistent in intensity for each form of the protein (Fig. 4).[37,50,55,58,59,62–67] These two bands are consistent in predominantly α-helical proteins, which lack β-sheet structure and have only minimal contributions from disordered structures.[43] In addition, these bands are dominant in the amide III region when contributions from disordered structures are eliminated, such as with the addition or organic modifiers[58] or by employing multivariate analysis methods.[50] Correlatively, the amide II mode in α-helical protein spectra typically exhibits two peaks at approximately 1511 and 1550–1560 cm^{-1}.[58] In the HP7 spectra, these peaks appear at about 1496 and 1540 cm^{-1}, respectively, which is consistent with the downshift that would be observed in an α-helical spectrum upon ^{15}N labeling (Fig. 3). In all three HP7 spectra, the component at 1496 cm^{-1} remains at a constant intensity and position. Last, all three spectra have a similar amide I shift of 1668 cm^{-1}. The constant peak positions of all modes in each of the HP7 spectra, as well as nearly identical intensities of the amide III bands at 1301 and 1335 cm^{-1}, are strong evidence for persistent α-helical content in each form of HP7.

Tertiary structural changes from the ordered to MG states

While the CD spectra of each form of HP7 display a similar amount of α-helical content, they do not exhibit equal amounts of disorder. In fact, while each spectrum contains a minimum at 222 nm, the minimum at 205 nm shifts approximately 2 nm upon each successive heme coordination to 209 nm for FHP7 (Fig. 1). Concurrently, the intensity of the maximum around 195 nm increases. These shifts and accompanying changes in intensity are consistent with an increase in disordered structure. While all forms are predominantly helical, consistent with the standard definition of a MG state, the precise nature of the helical and inter-helical domains distribution of structural order in each state remains an open question.

The dUVRR spectra of the model HP7 MG to ordered transition, are wholly consistent with observations from CD spectra that disorder is decreasing overall. Lack of shifts or changes in intensity of the amide III bands at 1301 and 1335 cm^{-1} suggest that the spectral changes are derived from greater restriction of motion in the inter-helical region, not changes in helical structure. The motion of each helix in relation to the others, or the gross tertiary structure, will have unique consequences for the types of structure that the inter-helical regions can explore. The amide III_3 (N–H bending, intra-residue C_α–N stretching, and some C_α–C stretching) and S modes (in-plane coupling of the N–H and C_α–H bending modes) are sensitive to local conformational distributions of individual backbone residues.[33,35] Therefore, in this case, these modes (amide III_3 and S) are likely reporting upon changes in the inter-

helical region that are associated with successive heme binding. The intensity of the amide S mode is positively correlated with non-helical structure.[33,35,55] As previously stated, the amide S mode relies on the coupling of the N–H and C_α–H bending modes of the protein backbone. In helical structures, the N–H and C_α–H moieties are trans to each other, un-coupling their vibrational motions and leading to a loss of intensity.[60] The dUVRR spectra following the transition from AHP7 to FHP7 reveal that the amide S mode decreases with each successive heme binding event. Thus, some population of amino acid residues within the inter-helical regions have ϕ/ψ angle distributions that allow for in-plane alignment and coupling of the bending motions of the C_α–H and N–H moieties, indicating the presence of non-helical dihedral angle sampling in these regions.

DUVRR spectral contributions in the amide III_3 mode are well correlated with specific types of structure found within a disordered protein.[44] Difference spectra obtained from the amide III_3 region clearly indicate two structural transitions that occur during each consecutive heme binding to HP7 (Fig. 5), which must correlate to non-helical structural sampling, as the helical mode intensities do not change. Therefore, the transition from the AHP7 state to HHP7 state causes a loss of extended-strand structure in the inter-helical regions, while the HHP7 to FHP7 transition corresponds to a loss in extended helical structure subsequent to the second heme binding based on the calculated psi angles for each wavenumber. Each of these transitions can be attributed to the binding of the heme groups, which limits the angles explored by the connecting regions between the helices. There is an equilibrium in the HP7 maquette between various tertiary structural populations, ranging from a compact state, with the helices closely bound by protein–protein interactions, to a more flexible, larger volume conformation. It is therefore reasonable to assume that when no heme is bound in the AHP7 form, the helices are free to undergo translational and rotational motion, allowing both inter-helical regions to explore a 'stretched-out' extended structure (Fig. 6). When a single heme is bound, the restriction of one inter-helical region shifts the protein towards a state that promotes protein–protein interactions, likely limiting the motion of both inter-helical regions. The second heme coordination fixes the four-helix bundle together, further shifting the equilibrium towards the more compact conformation.

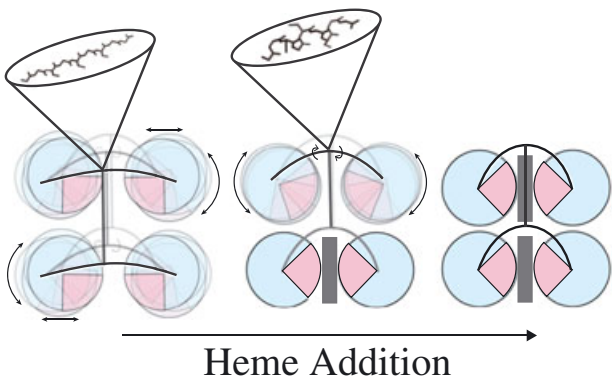

Figure 6. Schematic showing the disorder types of the inter-helical loops that are diminished during the stepwise transition from a molten globule to ordered state of the HP7. Insets represent the various types of extended structure observed in each form the protein. The colors of the helices represent the hydrophilic (blue) and hydrophilic (pink) regions, and the heme groups are represented in grey. This figure is available in colour online at wileyonlinelibrary.com/journal/jrs

The interactions fixing the orientation of the helices likely restrict the rotational freedom around each amide moiety in the inter-helical chain. This effectively reduces the global sampling of the ψ angles by residues within this region. Thus, in the dUVRR spectra, we see a loss in the amide III_3 intensity associated with these types of structure (Fig. 4). This is further supported by the increase in intensity of the phenylalanine modes in the dUVRR spectra (1000, 1028, 1609 cm^{-1}), which are known to increase concomitantly with an increase in the hydrophobic environment. The eight phenylalanine residues are oriented towards the interior of the four helix bundle in the ordered state.[46] The increased intensity of these modes with each heme binding event suggests each addition of heme brings the helices in closer proximity to each other, forming a more hydrophobic environment around the phenylalanine residues. This spectral trend further supports the idea of a shift in the equilibrium from an extended to a compact structure as a function of heme binding.

Like the amide S, the amide II mode is also expected to decrease in intensity in α-helical spectra.[33,35,68] The intensity and position of the α-helix related band at 1513 cm^{-1} are constant. The component at 1545 cm^{-1}, however, varies inversely with the rigidity of the peptide. Like the amide III_3 and S bands, the amide II intensity relies in part on the hypochromism associated with α-helical portions of protein spectra.[69] For a protein with more freedom of motion, the major component of the amide II mode, much like the III_3 and S, indicates that there is an increase in the disorder or conformational distribution at some positions within HP7, despite the appearance of persistent average α-helical character over time.

Conclusions

Results obtained using dUVRR of a model ordered to MG transition are consistent with previous data on HP7, showing that it retains its helical structure regardless of heme binding. Here, we present evidence that dUVRR spectroscopy can not only quantify the secondary structure content of the ordered state of the protein, but can also describe tertiary structural changes. This study represents the first detailed analysis of the MG state in which persistent secondary structure is observed, as well as the first application of dUVRR to the analysis of changes in tertiary structure in a protein of this size and physiological relevance, without changes in pH, temperature, or solvent. These results are promising evidence for the potential of dUVRR spectroscopy to monitor both secondary structural content and subtle local disorder simultaneously. It also offers insight into the effects of large-scale motion on local secondary structure.

Author contributions

The manuscript was written through contributions of all authors. All authors have given approval to the final version of the manuscript.

Acknowledgements

RLK gratefully acknowledges support by the following grants: FA9550-10-1-0350 from the Air Force Office of Scientific Research, infrastructure support from P41 GM-66354 to the New York Structural Biology Center and the NIH National Center for Research Resources to CCNY (NIH 5G12 RR03060). ACM gratefully

acknowledges support from the Center for Exploitation of Nanostructures in Sensor and Energy Systems (CENSES) under NSF Cooperative Agreement Award Number 0833180. RDJ gratefully acknowledges support from the NSF CAREER Award 1151533. The authors would also like to thank Professor Robert E. Blankenship, Departments of Chemistry and Biology, Washington University, for the use of the CD spectrometer.

References

[1] D. A. Dolgikh, Gilmanshin, R. I., Brazhnikov, E. V., Bychkova, V. E., Semisotnov, G. V., Venyaminov, S. Y., Ptitsyn, O. B., *FEBS Lett.* **1981**, *136*, 311.
[2] O. B. Ptitsyn, in Protein Folding (Ed.: T. E. Creighton), W. H. Freeman and Company, New York, NY, **1992**, pp. 243.
[3] O. B. Ptytsin, *Adv. Protein Chem.* **1995**, *47*, 83.
[4] V. E. Bychkova, Ptytsin, O. B., *Chemtracts Biochem. Mol. Biol.* **1993**, *4*, 133.
[5] M. Ohgushi, Wada, A., *FEBS J.* **1983**, *164*, 21.
[6] O. B. Ptitsyn, R. H. Pain, G. V. Semisotnov, E. Zerovnik, O. I. Razgulyaev, *FEBS J.* **1990**, *262*, 20.
[7] H. S. Bose, R. M. Whittal, M. A. Baldwin, W. L. Miller, *Proc. Natl. Acad. Sci. USA* **1999**, *96*, 7250.
[8] V. E. Bychkova, R. H. Pain, O. B. Ptytsin, *Biochemistry* **1992**, *31*, 7566.
[9] V. E. Bychkova, A. E. Dujsekina, S. I. Klenin, E. I. Tiktopulo, V. N. Uversky, O. B. Ptitsyn, *Biochemistry* **1996**, *35*, 6058.
[10] J. Martin, T. Langer, R. Boteva, A. Shramel, A. L. Horwich, F. U. Hartl, *Nature* **1991**, *352*, 36.
[11] F. G. Van der Goot, J. M. Gonzalez-Manas, J. H. Lakey, F. Pattus, *Nat. Struct. Biol.* **1991**, *354*, 408.
[12] S. M. Van der Vies, P. V. Viitanen, A. A. Gatenby, G. H. Lorimer, R. Jaenicke, *Biochemistry* **1992**, *31*, 3635.
[13] K. A. Crowhurst, M. Tollinger, J. D. Forman-Kay, *J. Mol. Biol.* **2002**, *322*, 163.
[14] K. A. Crowhurst, J. D. Forman-Kay, *Biochemistry* **2003**, *42*, 8687.
[15] M. Jeng, S. W. Englander, G. A. Elove, A. J. Wand, H. Roder, *Biochemistry* **1990**, *29*, 10433.
[16] S. Kristjansdottir, K. Lindorff-Larsen, W. Fieber, C. M. Dobson, M. Vendruscolo, F. M. Poulsen, *J. Mol. Biol.* **2005**, *347*, 1053.
[17] K. Lindorff-Larsen, S. Kristjansdottir, K. Teilum, W. Fieber, C. M. Dobson, F. M. Poulsen, M. Vendruscolo, *J. Am. Chem. Soc.* **2004**, *126*, 3291.
[18] T. K. Mal, S. J. Matthews, H. Kovacs, I. D. Campbell, J. Boyd, *J. Biomol. NMR* **1998**, *12*, 259.
[19] T. Mittag, J. D. Forman-Kay, *Curr. Opin. Struct. Biol.* **2007**, *17*, 3.
[20] P. J. R. Spooner, A. Watts, *Biochemistry* **1991**, *30*, 3871.
[21] D. K. Wilkins, S. B. Grimshaw, V. Receveur, C. M. Dobson, J. A. Jones, L. J. Smith, *Biochemistry* **1999**, *38*, 16424.
[22] J. D. Cortese, A. L. Voglino, C. R. Hackenbrock, *Biochemistry* **1998**, *37*, 6402.
[23] A. A. Deniz, T. A. Laurence, G. S. Beligere, M. Dahan, A. B. Martin, D. S. Chemla, P. E. Dawson, P. G. Schultz, S. Weiss, *Proc. Natl. Acad. Sci. USA* **2000**, *97*, 5179.
[24] T. Heimburg, D. Marsh, *Biophys. J.* **1993**, *65*, 2408.
[25] P. Hidlebrandt, T. Heimburg, D. Marsh, G. L. Powell, *Biochemistry* **1990**, *29*, 1661.
[26] K. Moncoq, I. Broutin, C. T. Craescu, P. Vachette, A. Ducruix, D. Durand, *Biophys. J.* **2004**, *87*, 4056.
[27] A. Muga, H. H. Mantsch, W. K. Surewicz, *Biochemistry* **1991**, *30*, 7219.
[28] T. J. T. Pinheiro, G. A. Elove, A. Watts, H. Roder, *Biochemistry* **1997**, *36*, 13122.
[29] N. Sanghera, T. J. T. Pinheiro, *Protein Sci.* **2000**, *9*, 1194.
[30] O. Tcherkasskaya, O. B. Ptytsin, *Protein Eng.* **1999**, *12*, 485.
[31] O. Tcherkasskaya, O. B. Ptytsin, *FEBS Lett.* **1999**, *455*, 325.
[32] Z. Zhang, D. L. Smith, *Protein Sci.* **1993**, *2*, 522.
[33] J. C. Austin, T. Jordan, T. G. Spiro, in Biomolecular Spectroscopy, Part A (Eds: R. J. H. Clark, R. E. Hester), John Wiley & Sons Ltd., New York, **1993**, p. 55.
[34] R. J. H. Clark, Spectroscopy of Biological Systems, Vol. 13, John Wiley & Sons Ltd., Chichester, **1986**.
[35] I. Harada, H. Takeuchi, in Spectroscopy of Biological Systems (Eds: R. J. H. Clark, R. E. Hester), John Wiley & Sons Ltd., New York, **1986**, p. 113.
[36] C. A. Roach, J. V. Simpson, R. D. JiJi, *Analyst* **2012**, *137*, 555.
[37] S. A. Oladepo, K. Xiong, Z. Hong, S. A. Asher, J. Handen, I. K. Lednev, *Chem. Rev.* **2012**, *112*, 2604.
[38] M. Ibrahim, R. L. Kerby, M. Puranik, I. H. Wasbotten, H. Youn, G. P. Roberts, T. G. Spiro, *J. Biol. Chem.* **2006**, *281*, 29165.
[39] J. Kneipp, G. Balakrishnan, T. G. Spiro, *J. Phys. Chem. B* **2004**, *108*, 15919.
[40] K. R. Rodgers, C. Su, S. Subramaniam, T. G. Spiro, *J. Am. Chem. Soc.* **1992**, *114*, 3697.
[41] T. Jordan, J. C. Eads, T. G. Spiro, *Protein Sci.* **1995**, *4*, 716.
[42] S. A. Asher, A. V. Mikhonin, S. Bykov, *J. Am. Chem. Soc.* **2004**, *126*, 8433.
[43] A. V. Mikhonin, Z. Ahmed, A. Ianoul, S. A. Asher, *J. Phys. Chem. B* **2004**, *108*, 19020.
[44] A. V. Mikhonin, S. V. Bykov, N. S. Myshakina, S. A. Asher, *J. Phys. Chem. B* **2006**, *110*, 1928.
[45] C. Halsey, J. Xiong, O. Oshokoya, J. Johnson, S. Shinde, T. J. Beaty, G. Ghirlanda, R. JiJi, J. Cooley, *Chembiochem* **2011**, *12*, 2125.
[46] R. L. Koder, K. G. Valentine, J. Cerda, D. Noy, K. M. Smith, J. A. Wand, P. L. Dutton, *J. Am. Chem. Soc.* **2006**, *128*, 14450.
[47] G. Balakrishnan, Y. Hu, S. B. Nielsen, T. G. Spiro, *Appl. Spectrosc.* **2005**, *59*, 776.
[48] J. R. Ferraro, K. Nakamoto, C. V. Brown, Introductory Raman Spectroscopy, (2 edn), Academic Press, San Diego, CA, **1994**.
[49] J. V. Simpson, O. Oshokoya, N. Wagner, J. Liu, R. D. JiJi, *Analyst* **2011**, 136, 1239.
[50] J. V. Simpson, G. Balakrishnan, R. D. JiJi, *Analyst* **2009**, *134*, 138.
[51] Y. H. Chen, J. T. Yang, H. M. Martinez, *Biochemistry* **1972**, *11*, 4120.
[52] G. Holzwarth, P. Doty, *J. Am. Chem. Soc.* **1965**, *87*, 218.
[53] P. A. Jennings, P. E. Wright, *Science* **1993**, *262*, 892.
[54] Y. Wang, R. Purrello, S. Georgiou, T. G. Spiro, *J. Am. Chem. Soc.* **1991**, *113*, 6368.
[55] Y. Wang, R. Purrello, T. Jordan, T. G. Spiro, *J. Am. Chem. Soc.* **1991**, *113*, 6359.
[56] X. G. Chen, R. Schweitzer-Stenner, S. Krimm, N. Mirkin, S. A. Asher, *J. Am. Chem. Soc.* **1994**, *114*, 11141.
[57] S. Krimm, J. Bandekar, in Advances in Protein Chemistry (Eds.: C. Anfinson, J. T. Edsall, F. M. Richards), Academic Press, New York, **1986**, p. 181.
[58] R. D. JiJi, G. Balakrishnan, Y. Hu, T. G. Spiro, *Biochemistry* **2006**, *45*, 34.
[59] S. A. Oladepo, K. Xiong, Z. Hong, S. A. Asher, *J. Phys. Chem. Lett.* **2011**, *2*, 334.
[60] S. A. Asher, A. Ianoul, G. Mix, M. N. Boyden, A. Karnoup, M. Diem, R. Schweitzer-Stenner, *J. Am. Chem. Soc.* **2001**, *123*, 11775.
[61] A. V. Mikhonin, N. S. Myshakina, S. V. Bykov, S. A. Asher, *J. Am. Chem. Soc.* **2005**, *127*, 7712.
[62] G. Balakrishnan, Y. Hu, G. M. Bender, Z. Getahun, W. F. DeGrado, T. G. Spiro, *J. Am. Chem. Soc.* **2007**, *129*, 12801.
[63] L. Ma, Z. Ahmed, A. V. Mikhonin, S. A. Asher, *J. Phys. Chem. B* **2007**, *111*, 7675.
[64] A. V. Mikhonin, S. A. Asher, *J. Phys. Chem. B* **2004**, *109*, 3047.
[65] A. V. Mikhonin, S. A. Asher, *J. Am. Chem. Soc.* **2006**, *128*, 13789.
[66] A. V. Mikhonin, S. A. Asher, S. V. Bykov, A. Murza, *J. Phys. Chem. B* **2007**, *111*, 3280.
[67] B. Sharma, S. V. Bykov, S. A. Asher, *J. Phys. Chem. B* **2008**, *112*, 11762.
[68] R. Schweitzer-Stenner, *Vib. Spectrosc* **2006**, *42*, 98.
[69] I. Tinoco, A. Halpern, W. T. Simpson, Polyamino Acids, Peptides, and Proteins, University of Wisconsin Press, Madison, WI, **1962**.